

Fermi Surface and Band Dispersion in $\text{La}_{2-x}\text{Sr}_x\text{CuO}_4$

A. Ino,¹ C. Kim,² T. Mizokawa,¹ Z.-X. Shen,² A. Fujimori,¹ M. Takaba,³ K. Tamasaku,³ H. Eisaki,³ and S. Uchida³

¹ Department of Physics, University of Tokyo, Bunkyo-ku, Tokyo 113-0033, Japan

² Department of Applied Physics and Stanford Synchrotron Radiation Laboratory, Stanford University, Stanford, CA94305, U.S.A.

³ Department of Superconductivity, University of Tokyo, Bunkyo-ku, Tokyo 113-0033, Japan

(September 24, 2018)

Using angle-resolved photoemission spectroscopy (ARPES), we have observed the band structure, Fermi surface and their doping dependences in $\text{La}_{2-x}\text{Sr}_x\text{CuO}_4$. The results reveal that the Fermi surface undergoes a dramatic change: it is hole-like and centered at $\mathbf{k} = (\pi, \pi)$ in underdoped ($x = 0.1$) and optimally doped ($x = 0.15$) samples as in other cuprates while it is electron-like and centered at (0,0) in heavily overdoped ($x = 0.3$) ones. The peak in the ARPES spectra near $(\pi/2, \pi/2)$ is broad and weak unlike in other cuprates. In the underdoped and optimally doped samples, a superconducting gap ($\Delta = 10 - 15$ meV) is observed on the Fermi surface near $(\pi, 0)$.

PACS numbers: 74.25.Jb, 71.18.+y, 74.72.Dn, 79.60.Bm

Among the family of high- T_c cuprate superconductors, $\text{La}_{2-x}\text{Sr}_x\text{CuO}_4$ (LSCO) provides unique opportunities to study the systematic evolution of the electronic structure with hole doping. First, LSCO has a simple crystal structure with single CuO_2 layers. It has no Cu-O chains as in $\text{YBa}_2\text{Cu}_3\text{O}_{7-\delta}$ (YBCO) nor complicated structural modulation of the block layers as in $\text{Bi}_2\text{Sr}_2\text{CaCu}_2\text{O}_{8+\delta}$ (Bi2212). Second, the hole concentration in the CuO_2 plane can be controlled in a wide range and uniquely determined by the Sr concentration x (and the small oxygen non-stoichiometry). One can therefore investigate the doping dependence of the electronic structure continuously from the heavily overdoped limit ($x \sim 0.35$) to the undoped insulator ($x = 0$) in the same system. This information should be highly useful to critically check existing theories of electron correlations and superconductivity in the CuO_2 plane. Indeed the doping dependences of thermodynamic and transport properties have been extensively studied for the LSCO system [1–4].

Angle-resolved photoemission spectroscopy (ARPES) is a powerful method to probe the electronic structure of low-dimensional systems. Particularly band structures, Fermi surfaces [5–10] and superconducting and normal-state gaps in the high- T_c cuprates [11–17] have been observed by ARPES. However, most of ARPES experiments were focused on the Bi2212 system and its family compounds; ARPES studies of LSCO have been hindered probably because LSCO is hard to cleave and its surface is not so stable as compared to the extremely stable surfaces of Bi2212 under an ultra-high vacuum.

We have recently focused on the LSCO system and carried out a series of photoemission studies [18,19]. Angle-integrated photoemission (AIPES) spectra of LSCO have shown a broad feature (at ~ -100 meV) and a suppression of the density of states at the Fermi level (E_F) in the underdoped region [19]. In the present study, we have overcome the experimental difficulties in the ARPES of LSCO using high-quality single crystals and

measured ARPES spectra of underdoped ($x = 0.1$), optimally doped ($x = 0.15$) and heavily overdoped ($x = 0.3$) samples in order to investigate the doping dependence of the electronic structure of the CuO_2 plane, in particular, the shape of the Fermi surface and the band dispersions.

Single crystals of LSCO ($x = 0.1, 0.15$ and 0.3) were grown by the traveling-solvent floating-zone method. The ARPES measurements were carried out at beamline 5-3 of Stanford Synchrotron Radiation Laboratory (SSRL), using incident photons with energies of 22.4 eV and 29 eV. The wave vector and the electric vector of the incident photons and the sample surface normal were kept in the same plane and an angle of incidence was 45° . The total energy resolution was approximately 45 meV and the angular resolution was ± 1 degree. The spectrometer was kept in an ultra high vacuum better than 5×10^{-11} Torr during the measurements and the samples were cleaved *in situ*. Since the surface degraded rapidly at high temperatures, the measurements were done only at low temperatures ($T \sim 15$ K). The cleanliness of the surface was checked by the absence of a hump at energy ~ -9.5 eV and a shoulder in the valence band at ~ -5 eV. All the spectra presented here were taken within 10 hours and mostly 5 hours after cleaving. The position of the Fermi level was calibrated with gold spectra for every measurement and the experimental uncertainty of the energy calibration was about ± 2 meV.

ARPES spectra for underdoped ($x = 0.1$) and optimally doped ($x = 0.15$) LSCO are shown in Fig. 1. Although the dispersive features are broad, an angular dependence is identified. As one goes from (0,0) to $(\pi, 0)$ in the first Brillouin zone (BZ) or from $(2\pi, 0)$ to $(\pi, 0)$ in the second BZ [Figs. 1(a) and (b)], a broad “quasiparticle” (QP) peak emerges from lower energies and then stays somewhat below E_F around the $(\pi, 0)$ point, never crossing the Fermi surface. The midpoint of the leading edge is below E_F (~ -20 meV) at $\sim (\pi, 0)$. As for Fig. 1(b), the peak intensity decreases in going from $(1.2\pi, 0)$ to

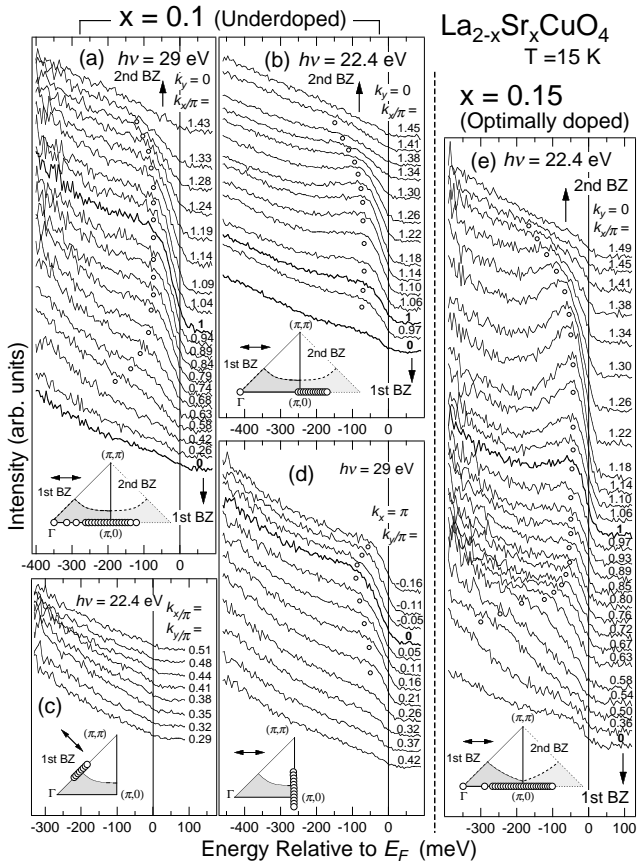


FIG. 1. ARPES spectra of underdoped ($x = 0.1$) and optimally doped ($x = 0.15$) $\text{La}_{2-x}\text{Sr}_x\text{CuO}_4$ near the Fermi level. Insets show measured points in the momentum space and the polarization of incident photons (arrows).

$(\pi,0)$. This is probably due to a matrix-element effect peculiar to the incident photon energy of $h\nu = 22.4 \text{ eV}$ because such an intensity modulation is not seen in the spectra taken at another photon energy $h\nu = 29 \text{ eV}$ as shown in Fig. 1(a). The dispersion of the QP peak is very weak around the $(\pi,0)$ point, meaning that there is a “flat band”, namely, an extended saddle-point around $(\pi,0)$ as in other cuprates [7]. On the other hand, as one goes from $(\pi,0)$ towards (π,π) [Fig. 1(d)], the broad peak and its leading edge further approach E_F and then the peak disappears around $\sim(\pi,0.2\pi)$. Since a superconducting gap is opened on the Fermi surface at this temperature ($T \sim 15 \text{ K} < T_c$), the leading-edge midpoint stays below E_F ($\sim -8 \text{ meV}$) even for the peak closest to E_F . It has been indeed reported that the minimum-gap locus in the superconducting state coincides with the Fermi surface in the normal state [20]. Therefore, we may conclude that the band crosses an underlying Fermi surface around $\sim(\pi,0.2\pi)$. As for the $(0,0) \rightarrow (\pi,\pi)$ cut [Fig. 1(c)], no QP peak is identified in the present spectra. However, the fact that the QP band is below E_F at $(\pi,0)$ implies that the Fermi surface underlying the superconducting gap is hole-like and centered at (π,π) for

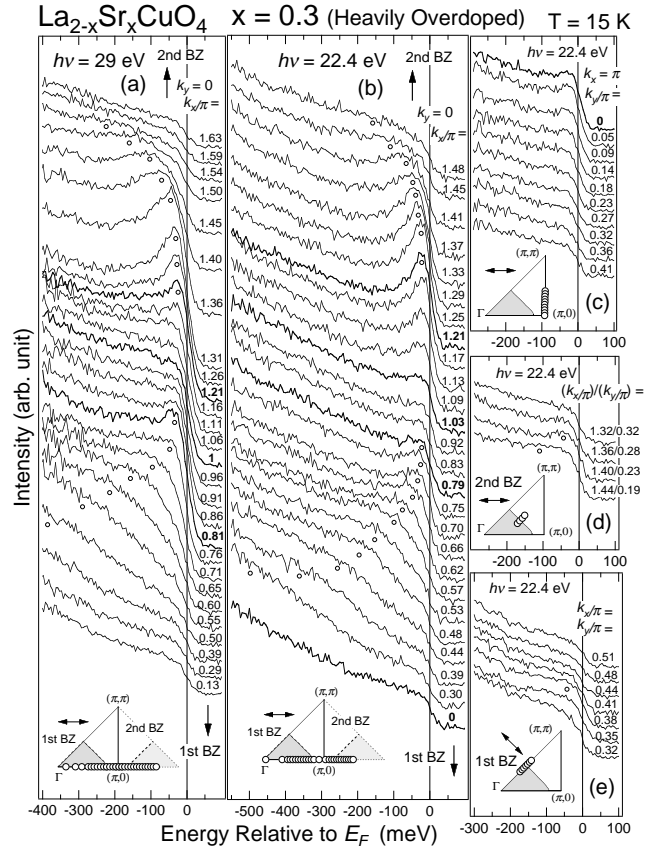


FIG. 2. ARPES spectra of heavily overdoped ($x = 0.3$) $\text{La}_{2-x}\text{Sr}_x\text{CuO}_4$ near the Fermi level. Insets show measured points in the momentum space and the polarization of incident photons (arrows).

$x = 0.1$ as in other cuprates studied previously such as Bi2212 , Bi2201 , YBCO and $\text{Nd}_{2-x}\text{Ce}_x\text{CuO}_4$ [6–10].

Spectra for $x = 0.15$ showed a behavior similar to $x = 0.1$: the QP peak and the leading-edge midpoint stay below E_F in $(0,0) \rightarrow (\pi,0)$ as shown in Fig. 1(e) and the peak disappears in going from $(\pi,0)$ to (π,π) , indicating a hole-like underlying Fermi surface as in $x = 0.1$. The leading-edge midpoint reaches about -3 meV at the closest to E_F . The peak intensity is pronounced around $(1.2\pi,0)$ because of the matrix-element effect peculiar to $h\nu = 22.4 \text{ eV}$ as in $x = 0.1$ [Fig. 1(b)] and some of other cuprates [8]. Note, however, that no decrease in the peak intensity is found in $\sim(0.8\pi,0) \rightarrow (\pi,0)$ in the first BZ for $x = 0.15$.

ARPES spectra for heavily overdoped ($x = 0.3$) LSCO are shown in Fig. 2. Going from $(0,0)$ to $(\pi,0)$ or from $(2\pi,0)$ to $(\pi,0)$ [Figs. 2 (a) and (b)], the QP peak moves upwards, reaches E_F around $\sim(0.8\pi,0)$ and $\sim(1.2\pi,0)$, then decreases in its intensity both in the first and second BZ and almost disappears at $(\pi,0)$ both in the spectra taken at $h\nu = 29 \text{ eV}$ and $h\nu = 22.4 \text{ eV}$. Here the leading-edge midpoint also reaches $\sim +6 \text{ meV}$ above E_F at $\sim(1.2\pi,0)$, suggesting that the QP band has in-

deed reached the Fermi level. That should be contrasted with the overdoped Bi2212, where the leading-edge midpoint goes above E_F to the same extent for the Fermi-surface crossing near $(\pi/2, \pi/2)$ and is always below E_F in $(0,0) \rightarrow (\pi,0)$ [13,22]. Meanwhile, since the matrix-element effect is dependent on the energy of incident photons and different between the first and second BZ, it would be unlikely that all of the intensity decrease at $\sim(0.8\pi,0)$ and $\sim(1.2\pi,0)$ is due to the matrix-element effect. Indeed, for the spectra taken at $h\nu = 29$ eV, both the intensity decrease at $\sim(0.8\pi,0)$ and $\sim(1.2\pi,0)$ observed for $x = 0.3$ [Fig. 2 (a)] are not found for $x = 0.1$ [Fig. 1 (a)], distinguishing the two compositions. Furthermore, in contrast to the spectra for $x = 0.15$ taken at $h\nu = 22.4$ eV [Fig. 1 (e)], the QP peak seen at $(0.75\pi,0)$ almost disappears at $(0.92\pi,0)$ in the first BZ for $x = 0.3$ [Fig. 2 (b)]. Therefore, we have concluded that the QP band crosses the Fermi surface around $(0.8\pi,0)$ for $x = 0.3$. A close inspection of the spectra [Figs. 2 (b) and (c)] reveals that part of the QP peak weight appears to remain below E_F at $\sim(\pi,0)$, suggesting that the “flat band” stays only slightly above E_F at $(\pi,0)$. In the presence of strong electron correlation, the QP peak is no more a single peak and part of the spectral weight is distributed on the other side of E_F . This also explains the intensity drop in going from $(\pi,0)$ to (π,π) as seen in Fig. 2 (c). Along the $(0,0) \rightarrow (\pi,\pi)$ cut [Fig. 2(d)], although the peak is not clearly identified, the edge intensity slightly increases at $\sim(0.38\pi, 0.38\pi)$ and then drops at $\sim(0.44\pi, 0.44\pi)$, a behavior indicative of a Fermi-surface crossing. This intensity variation was reproduced in several measurements. The QP peak near $(\pi/2, \pi/2)$ is broad and weak compared to the peak near $(\pi,0)$ in contrast to other cuprates showing clear QP peaks around $(\pi/2, \pi/2)$ [6,12,13,21]. To summarize, the observations indicate that the Fermi surface is electron-like and centered at the $(0,0)$ point for $x = 0.3$ unlike the other cuprates studied so far.

Thus the Fermi surface undergoes a dramatic change from hole-like to electron-like between $x = 0.15$ and $x = 0.3$, as the flat band around $(\pi,0)$ moves from below E_F to above E_F . The change in the Fermi-surface topology may be related to the observation that the sign of the Hall coefficient changes from positive to negative around $x = 0.25$ in LSCO [23,24] and has the same tendency as what is expected from the local-density-approximation (LDA) band-structure calculation of La_2CuO_4 by shifting the Fermi level as in the rigid band model [25,26]. The behavior of the $(\pi,0)$ flat band upon doping is consistent with numerical studies of the Hubbard model [27,28]. Figure 3 shows the Fermi surfaces suggested from the present experiments for $x = 0.1$ and 0.3 . The area enclosed by the Fermi surface is $71 \pm 3\%$ of the half BZ area for $x = 0.3$, which agrees well with the number of electrons $1 - x$ as expected from the Luttinger sum rule, indicating a “large Fermi surface”. As for $x = 0.1$, the Fermi

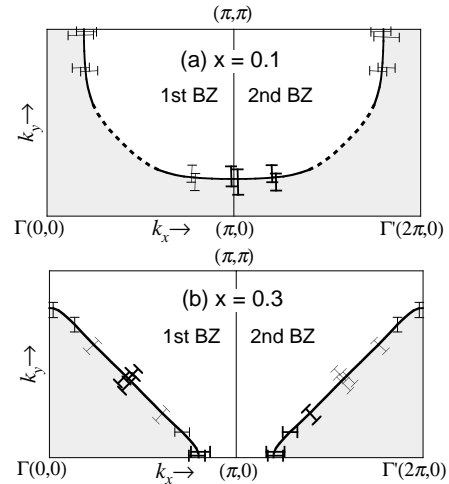


FIG. 3. Fermi surfaces of $\text{La}_{2-x}\text{Sr}_x\text{CuO}_4$ for $x = 0.1$ (a) and $x = 0.3$ (b). Observed Fermi-surface crossings are denoted by thick error bars. Thin error bars indicate Fermi-surface crossings folded by symmetry. As for $x = 0.1$, minimum-gap locus are taken as Fermi-surface crossings and dotted curve is tentatively drawn so that the area enclosed by the Fermi surface is $\sim 0.9(\pi^2/2)$.

surface near $(\pi/2, \pi/2)$ (dashed curve) has been tentatively drawn in Fig. 3 so that the enclosed area is consistent with the Luttinger sum rule. According to Fig. 3, the Fermi surface for $x = 0.3$ seems to be almost square and have a large straight portion around $(\pi/2, \pi/2)$. Recently, Fermi-surface nesting [29] and short-range stripe order [30] have been proposed as the origin of the incommensurate peaks in the dynamical magnetic structure factor $S(\vec{q}, \omega)$ observed by inelastic neutron scattering. However, the Fermi-surface nesting would not explain why the incommensurate peaks are smeared out in the overdoped region ($x > 0.25$) as recently observed [31] in the presence of the straight Fermi surface for $x = 0.3$.

The width of the QP peak around $(\pi,0)$ for LSCO is almost the same as that for Bi2212 with corresponding hole doping [6,12,13,21], even though the dispersive features are weaker for LSCO than for Bi2212. The QP peak becomes broader as x decreases from the overdoped to the underdoped regions. The broad peak on the flat band around $(\pi,0)$ may be related to the broad feature in the AIPES spectra, where the spectral intensity starts to decrease towards E_F in the underdoped LSCO [19], that is, what is called a high-energy pseudogap or a weak pseudogap [32] on an energy scale (~ 100 meV) much larger than the superconducting gap and the “normal-state gap” ($\lesssim 20$ meV) [13–17]. Both the broad $(\pi,0)$ peak in the ARPES spectra and the high-energy pseudogap in the AIPES spectra have nearly the same energy scales, that is, the order of the superexchange energy $J \sim 100$ meV and also increase in their energies as x decreases, following the development of antiferromagnetic correlations [19]. The QP peak lineshape and its doping

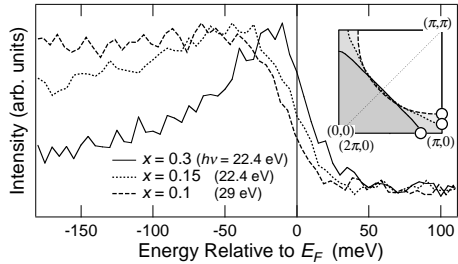


FIG. 4. ARPES spectra for momenta on the Fermi surface (minimum-gap locus) near $(\pi, 0)$ shown by open circles in the inset. For each composition x , the spectrum at $(0, 0)$ has been subtracted as the angle-independent background.

dependence in the $(0,0) \rightarrow (\pi,0)$ cut of LSCO is also consistent with the trend among Bi2212, $\text{Sr}_2\text{CuO}_2\text{Cl}_2$ and the $t - t' - t'' - J$ model calculation [21,33]. These observations suggest that the broad lineshape of the ARPES spectra around $(\pi,0)$ is originated from antiferromagnetic correlations.

The magnitude of the superconducting gap may be roughly estimated from the shift of the leading edge on the Fermi surface (Fig. 4) [15,16]. For the non-superconducting sample ($x = 0.3$), the leading-edge midpoint is pushed above E_F ($\sim +6$ meV) at the Fermi-surface crossing $\sim(1.2\pi, 0)$ due to the finite instrumental resolution (~ 45 meV). On the other hand, the leading-edge midpoint is below E_F , ~ -8 and ~ -3 meV for $x = 0.1$ and 0.15 , respectively, on the Fermi surface near $(\pi,0)$. Accordingly, the relative shift of the leading edge is about $10 - 15$ meV on the Fermi surface near $(\pi,0)$ for $x = 0.1$ and 0.15 , and is smaller than the typical value ~ 25 meV for Bi2212 and YBCO [13,15,17], but is similar to that of $\text{Bi}_2\text{Sr}_2\text{CuO}_{6+\delta}$ (Bi2201) [16], which also has single CuO_2 planes. These leading-edge shifts scale well with the maximum T_c of the systems. The superconducting gap of $\Delta = 10 - 15$ meV estimated here is roughly consistent with Raman scattering [34], tunneling [35] and neutrons [36] results on LSCO.

In conclusion, we have successfully observed band dispersions and Fermi surfaces in overdoped and underdoped LSCO. It is found that the hole-like underlying Fermi surface centered at (π, π) for $x = 0.1$ and 0.15 turns to the electron-like Fermi surface centered at $(0, 0)$ for $x = 0.3$ (heavily overdoped). The peak in ARPES spectra near $(\pi/2, \pi/2)$ is quite broad and weak compared to other cuprates. In the underdoped and optimally doped samples, a superconducting gap ($\Delta = 10 - 15$ meV) is observed on the Fermi surface at $\sim(\pi, 0.2\pi)$. More studies are necessary to identify the anisotropy, doping dependence and temperature dependence of the superconducting gap.

This work is supported by a Grant-in-Aid for Scientific Research from the Ministry of Education, Science, Sports and Culture of Japan, the New Energy and Industrial Technology Development Organization (NEDO), Special

Coordination Fund for Promoting Science and Technology from Science and Technology Agency of Japan, the U. S. DOE, Office of Basic Energy Science and Division of Material Science. Stanford Synchrotron Radiation Laboratory is operated by the U. S. DOE, Office of Basic Energy Sciences, Division of Chemical Sciences.

+ Present address: The Institute of Physical and Chemical Research (RIKEN), SPring-8, Kamigori-cho, Hyogo 678-12, Japan.

- [1] H. Takagi *et al.*, Phys. Lett. **69**, 2975 (1992).
- [2] T. Nakano *et al.*, Phys. Rev. B **49**, 16000 (1994).
- [3] H. Y. Hwang *et al.*, Phys. Rev. Lett. **72**, 2636 (1994).
- [4] J. W. Loram *et al.*, Physica C **162-164**, 498 (1989); N. Momono *et al.*, Physica C **233**, 395 (1994).
- [5] C. G. Olson *et al.*, Phys. Rev. B **42**, 381 (1990).
- [6] D. S. Dessau *et al.*, Phys. Rev. Lett. **71**, 2781 (1993); H. Ding *et al.*, Phys. Rev. Lett. **76**, 1533 (1996).
- [7] D. M. King *et al.*, Phys. Rev. Lett. **73**, 3298 (1994).
- [8] R. Liu *et al.*, Phys. Rev. B **46**, 11056 (1992).
- [9] R. Anderson *et al.*, Phys. Rev. Lett. **70**, 3163 (1993).
- [10] D. M. King *et al.*, Phys. Rev. Lett. **70**, 3159 (1993).
- [11] Z.-X. Shen *et al.*, Phys. Rev. Lett. **70**, 1553 (1993).
- [12] D. S. Marshall *et al.*, Phys. Rev. Lett. **76**, 4841 (1996).
- [13] A. G. Loeser *et al.*, Science. **273**, 325 (1996).
- [14] H. Ding *et al.*, Nature **382**, 51 (1996).
- [15] J. M. Harris *et al.*, Phys. Rev. B **54**, 15665 (1996).
- [16] J. M. Harris *et al.*, Phys. Rev. Lett. **79**, 143 (1997).
- [17] M. Schabel *et al.*, Phys. Rev. B **55**, 2796 (1997).
- [18] A. Ino *et al.*, Phys. Rev. Lett. **79**, 2101 (1997).
- [19] A. Ino *et al.*, Phys. Rev. Lett. **81**, 2124 (1998).
- [20] J. C. Campuzano *et al.*, Phys. Rev. B **53**, 14737 (1996).
- [21] Z.-X. Shen and J. R. Schrieffer, Phys. Rev. Lett. **78**, 1771 (1997).
- [22] D. S. Dessau *et al.*, Phys. Rev. B **45**, 5095 (1992).
- [23] K. Tamasaku *et al.*, Phys. Rev. Lett. **72**, 3088 (1994).
- [24] S. Uchida *et al.*, in *Strong Correlation and Superconductivity*, edited by H. Fukuyama, S. Maekawa and A. P. Malozemoff (Springer-Verlag, Berlin 1989), p. 194.
- [25] L. F. Mattheiss, Phys. Rev. Lett. **58**, 1028 (1987).
- [26] W. E. Pickett, Rev. Mod. Phys. **61**, 433 (1989).
- [27] D. Duffy *et al.*, Phys. Rev. B **56**, 5597 (1997).
- [28] R. Preuss *et al.*, Phys. Rev. Lett. **79**, 1122 (1997).
- [29] T. Tanamoto, H. Kohno and H. Fukuyama, J. of Phys. Soc. Jpn **61**, 1886 (1992).
- [30] J. M. Tranquada *et al.*, Nature **375** 561 (1995).
- [31] K. Yamada *et al.*, Phys. Rev. B **57** 6165 (1998).
- [32] J. Schmalian, D. Pines and B. Stojkovic, Phys. Rev. Lett. **80**, 3839 (1998).
- [33] C. Kim *et al.*, Phys. Lett. **80**, 4245 (1998).
- [34] X. K. Chen *et al.*, Phys. Rev. Lett. **73**, 3290 (1994).
- [35] T. Nakano *et al.*, J. Phys. Soc. Jpn. **67**, 2622 (1998).
- [36] K. Yamada *et al.*, Phys. Rev. Lett. **75**, 1626 (1995).